DOI: 10.1002/anie.200603402

With Phosphinophosphonic Acids to Nanostructured, Water-Soluble, and Catalytically Active Rhodium Clusters

Julija Glöckler, Stefan Klützke, Wolfgang Meyer-Zaika, Armin Reller, F. Javier García-García, Hans-Henning Strehblow, Petra Keller, Eva Rentschler, and Wolfgang Kläui*

Nanostructured metal clusters[1] are of great interest as catalysts for organic as well as inorganic reactions and especially as electrocatalysts for fuel cells. As components for materials with special electronic, optical, or magnetic properties they are regarded as a promising basis for entirely new branches of industry.

Metal clusters in the range of 1–4 nm are of special interest since this range covers the continuous transition of non-metallic compounds to the bulk metal.[1d,e] In this range the particles show size-dependent catalytic properties. The smaller the metal particles are, the higher the ratio of surface atoms to the total number of atoms. Therefore, small clusters often show especially high catalytic activity.[1f,2] Among other features, the ratio of the different types of surface atoms changes: with increasing particle size the proportion of terrace atoms increases whereas the proportion of atoms on edges (step atoms) and especially on vertices (kink atoms) decreases.[3] Monodisperse metal clusters in the range of 1–4 nm are ideally suited for a detailed analysis of the size dependence and selectivity of catalytic reactions. However, small clusters of this size tend to aggregate owing to their high specific surface and can generally only be stabilized in aqueous solution in the presence of surfactants or polymers.[1g,2,4,5] We have found a route leading to rhodium clusters with a very narrow particle size distribution. Their mean diameter is in the range 2–6 nm, depending on the reaction conditions. These clusters are water soluble, stable in air, stable in aqueous solution for months, and can be isolated as redispersible solids. The aqueous cluster solutions show high activity in the biphasic hydrogenation of olefins and are able to hydrogenate aromatic compounds. Complexes with sulfonated phosphane ligands are predominantly used as water-soluble rhodium catalysts.[6] We observed that the introduction of phosphonate substituents (PO_3^{2-}) leads to significantly higher water solubility than the introduction of sulfonate groups (SO_3^-). For example, the phosphane ligand $Na_2[Ph_2PCH_2CH_2PO_3]$ (Na_2-**1**) with just one phosphonate group is as water-soluble (ca. 1100 $g L)^{-1}$ as tppts, a triphenylphosphine with three sulfonate groups. The synthesis of Na_2-**1** is outlined in Scheme 1.

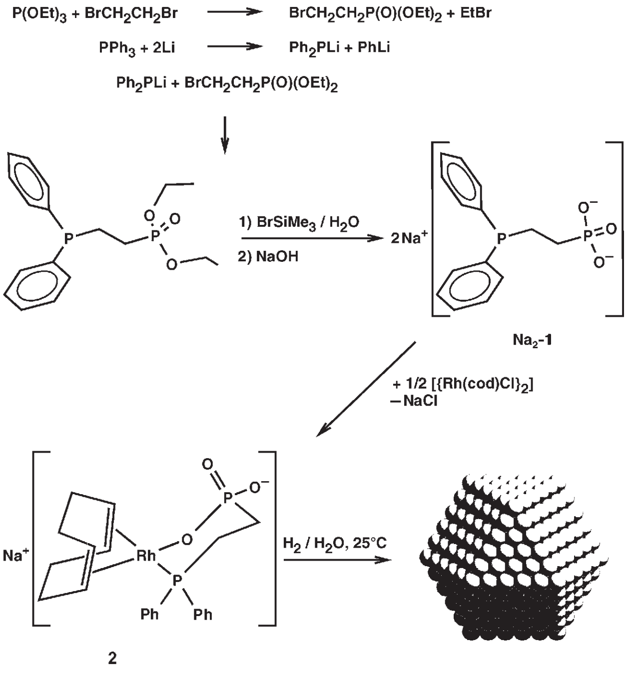

Scheme 1. Outline of the route that leads to phosphinophophonic acid-stabilized rhodium clusters (represented, in this case, as a five-shell "magic number" cluster consisting of 561 rhodium atoms).

Upon reaction of $[\{Rh(cod)Cl\}_2]$ (cod = cyclooctadiene) with Na_2-**1**, the water-soluble rhodium(I) complex **2** is formed with the phosphane ligand **1** acting as P,O-chelate ligand. Because of the low affinity of rhodium for oxygen-donor ligands we assumed that **1** could act as "hybrid ligand",[7] "hemilabile ligand",[8] or as "dangling ligand"[9] and therefore

---

[*] Dipl.-Ing. J. Glöckler, Dr. S. Klützke, Prof. Dr. W. Kläui
Institut für Anorganische Chemie und Strukturchemie
Lehrstuhl I: Bioanorganische Chemie und Katalyse
Heinrich-Heine-Universität Düsseldorf
Universitätsstrasse 1, 40225 Düsseldorf (Germany)
Fax: (+49) 8112287
E-mail: klaeui@uni-duesseldorf.de
Homepage: http://www.chemie.uni-duesseldorf.de/Faecher/Anorganische_Chemie/AC1/Klaeui/

Dr. W. Meyer-Zaika
Institut für Anorganische Chemie
Universität Duisburg-Essen, 45117 Essen (Germany)

Prof. Dr. A. Reller, Dr. F. J. García-García
Lehrstuhl für Festkörperchemie, Universität Augsburg
Universitätsstrasse 1, 86159 Augsburg (Germany)

Prof. Dr. H.-H. Strehblow, Dr. P. Keller
Institut für Physikalische Chemie und Elektrochemie 2
Heinrich-Heine-Universität Düsseldorf
Universitätsstrasse 1, 40225 Düsseldorf (Germany)

Prof. Dr. E. Rentschler
Institut für Anorganische Chemie und Analytische Chemie
Johannes-Gutenberg-Universität Mainz
Duesbergweg 10–14, 55128 Mainz (Germany)

Supporting information for this article is available on the WWW under http://www.angewandte.org or from the author.

would be ideally suited to provide an easily accessible coordination site in a catalytic cycle. However, preliminary experiments did not show any reaction of **2** with olefins in the presence of hydrogen gas. Instead we observed that after 3 days an aqueous solution of the rhodium complex **2** turned ink-black under atmospheric hydrogen pressure at room temperature. No rhodium metal precipitated, no rhodium mirror formed on the glass wall. A black solid is isolated upon evaporation of the solvent and can be redissolved in water yielding again a black solution. At higher hydrogen pressure in an autoclave black solutions are obtained after just a few hours. High-resolution TEM (HRTEM) images (Figure 1–3) show that these solutions contain rhodium clusters of remarkable narrow particle size distribution. The mean diameter depends upon the hydrogen pressure applied in the synthesis. At atmospheric pressure the mean diameter is 6 nm (Figure 1), at 30 bar 3 nm (Figure 2 a–c), and at 60 bar of hydrogen 2.5 nm (Figure 3). A diameter of approximately 2.4 nm corresponds to a five-shell "magic number" cluster of 561 rhodium atoms.

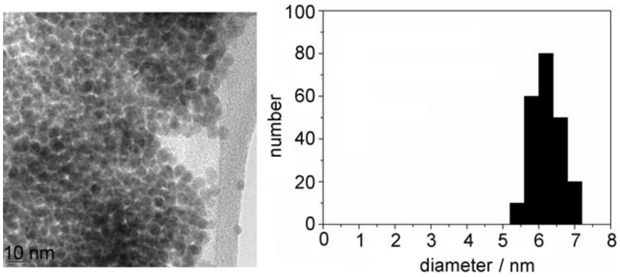

Figure 1. TEM image (left) of rhodium nanocrystals (6 nm) supported on amorphous carbon film and particle size distribution (right) of the clusters: (6.2 ± 0.4) nm.

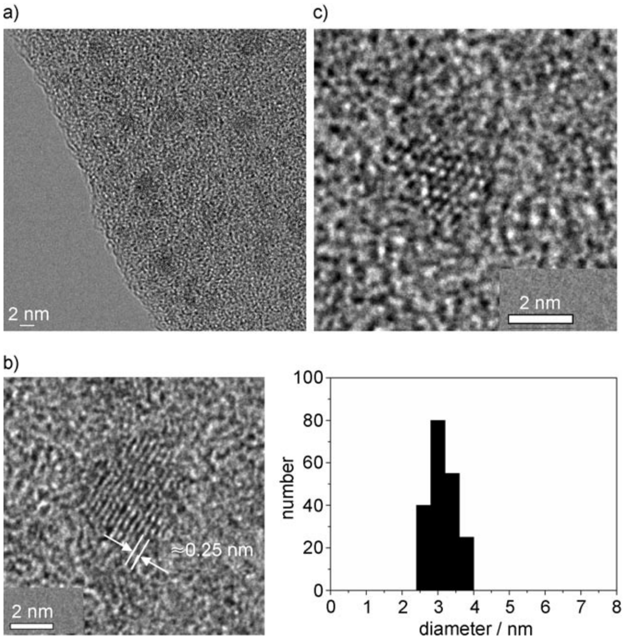

Figure 2. a) HRTEM image of rhodium nanocrystals supported on amorphous carbon film. The image shows that the nanocrystals do not agglomerate. b) HRTEM image (left) of a single 3-nm rhodium nanocrystal and particle size distribution (right) of the clusters: (3.1 ± 0.4) nm. The measured distances between the crystallographic planes are in accord with the Rh–Rh distances reported for rhodium metal. c) HRTEM image of a rhodium nanocrystal oriented in the [111] direction. In this case as well, the measured distances between contrast maxima and minima can be interpreted in terms of the structural data of metallic rhodium.

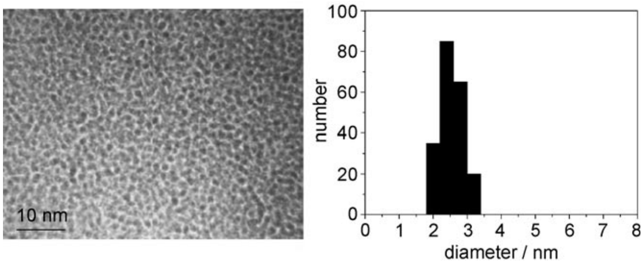

Figure 3. TEM image (left) of rhodium nanocrystals (2.5 nm) supported on amorphous carbon film and particle size distribution (right) of the clusters: (2.5 ± 0.4) nm.

We tried to further characterize the clusters. It seems reasonable to assume that ligands $\mathbf{1}^{2-}$ located on the surface of the clusters prevent coagulation through strong electrostatic repulsion.[10] Interestingly, the ^{31}P NMR spectrum of an aqueous cluster solution shows no signal for excess non-coordinated ligand $\mathbf{1}^{2-}$ but exclusively one for the corresponding phosphane oxide $[Ph_2P(O)CH_2CH_2PO_3]^{2-}$. It is clear that the phosphane ligand is oxidized upon cluster formation despite strict exclusion of oxygen and despite the presence of a hydrogen atmosphere! Patin et al. investigated the reduction of $RhCl_3{\cdot}3\,H_2O$ by tppts and showed that water is the source of oxygen in the phosphane oxidation reaction.[11]

Why in our case the phosphane ligand is converted into the phosphane oxide is not yet clear. Even if the reduction of the rhodium(I) complex **2** to give elemental rhodium is coupled to a stoichiometric oxidation of the phosphane ligand $\mathbf{1}^{2-}$, excess free phosphane ligand should still be observed. It is also remarkable that no phosphane ligands residing on the cluster surfaces are detected in the ^{31}P NMR spectrum. We therefore took a closer look at the magnetic properties of the clusters. The calculations and measurements made on the paramagnetism of "naked" clusters are contradictory. To our knowledge, no measurements on ligand-stabilized discrete clusters have been performed to date. In contrast to some 3d elements, no spontaneous magnetic ordering is observed with 4d or 5d elements. The magnetic behavior of the heavier homologues of the 3d elements, however, is determined by high spin-orbit coupling contributions. Thus such elements—once magnetized—could represent an especially interesting class of compounds with high magneto-crystalline anisotropy. Rhodium shows extraordinary magnetic properties within this group of elements. In the solid state it is nonmagnetic, yet in mono-atomic layers and discrete Rh_n clusters ($n = 6$–43) it shows astonishingly high magnetic moments. Depending on cluster size, magnetic moments of more than 1 μB per atom are reported, for example, for $n = 13$.[12] A consistent interpretation of the experimental data and theoretical calculations has not yet been reached owing to experimental difficulties. The 2-nm diameter rhodium clusters with their narrow particle size distribution that we have obtained could be suitable particles for studying magnetic properties. None of the samples, however, gave an indication of superparamagnetic behavior. The temperature dependence of the measured magnetic moments is dominated by diamagnetic contributions and contributions from spin-orbit coupling (see Supporting Information). In the group of clusters investigated the solid-state character clearly dominates over the surface properties. We are now looking for ways to get ligand-stabilized clusters in the subnanometer range.

The clusters presented herein are air stable and their catalytic hydrogenation activity is virtually independent of the presence of air. To date we have no information on the oxidation state of the rhodium surface atoms and whether oxide ions are present on the cluster surface. The characterization of cluster surfaces is a general problem which is very often not addressed. X-ray photoelectron spectroscopy (XPS) is a suitable method for analyzing surfaces. XPS provides information on the oxidation states of the detected elements when suitable reference standards are available. We used metallic rhodium and $RhCl_3{\cdot}3\,H_2O$ as references und determined the position of the Rh $3d_{5/2}$ line (see Supporting Information). The energies determined are in good agreement with the values found in the literature. The Rh $3d_{5/2}$ line of 6-nm rhodium clusters was determined to be at $E_B = 308.2$ eV, it is shifted by $\Delta E = 1$ eV relative to metallic rhodium. Clearly, the electronic structure of clusters, even of this size, is different from that of rhodium metal.[13] The reason for not being able to get any distinct information on the surface atoms of the clusters using XPS lies in the dimensions of the clusters. A wavelength of $\lambda = 3.29$ nm is calculated for the photoelectrons of the Rh $3d_{5/2}$ signal with $E_{kin} = 1179.2$ eV by using the relation $\lambda = 0.096\sqrt{E_{kin}}$.[14] This result means that XPS does not characterize the cluster surface but measures the electronic state of the whole cluster!

The HRTEM and electron diffraction data show that the rhodium clusters virtually exist as single crystals. The interplanar spacing according to the contrast maxima and electron diffraction diagrams are in accord with the structural data for metallic rhodium. Experiments using locally resolved element-specific energy-dispersive X-ray (EDX) analysis (EDAX system) give evidence for the presence of a phosphorus-containing ligand shell surrounding the rhodium nanoclusters.

The data on the catalytic activity of the clusters is shown in Table 1. All the experiments on biphasic catalysis were performed in a stainless steel autoclave with glass insert at elevated pressure. The results show that under the same conditions small clusters exhibit significantly higher catalytic activity than lager ones. The turn-over frequency (TOF) of the hydrogenation of 1-hexene catalyzed by 6-nm clusters at 20 bar of hydrogen is about 2100 h^{-1}. Under the same conditions, 3-nm clusters catalyze the hydrogenation of 1-hexene at a TOF of 3600 h^{-1}. The same trend is also seen in the hydrogenation of benzene. Nitrobenzene is reduced to aniline (TOF = 600 h^{-1} at 60 °C, 80 bar H_2-pressure, 3-nm clusters).

Table 1: Hydrogenation of 1-hexene and benzene at 20 °C using rhodium clusters of varying size as catalysts.

	1-Hexene		Benzene	
Cluster size [nm]	H_2 pressure [bar]	TOF [h^{-1}]	H_2 pressure [bar]	TOF [h^{-1}]
6.2	20	2100	20	1
3.1	20	3600	20	50
2.0	20	5700	20	80

Herein we have shown that the water-soluble rhodium(I) complex **2** can be reduced by hydrogen. In this reaction, rhodium clusters of narrow particle size distribution are formed which can be isolated and are redispersible in water without coagulation. The outstandingly high stability is caused by the electrostatic repulsion of the double negative charge of the phosphonate ligands covering the clusters. The mechanistic role of the phosphinophosphonic acid ligands in the reduction of rhodium is not fully understood, since more phosphane is oxidized to phosphane oxide than would be needed for the formal reduction of rhodium(I) to rhodium(0). The elucidation of the reaction mechanism and stabilization of water-soluble clusters of other metals by phosphinoposphonates are subject of current research.

Experimental Section

^1H and ^{31}P NMR spectra were recorded on a Bruker spectrometer DRX200, ^{13}C NMR spectra on a Bruker DRX500. For HRTEM imaging electron microscopes JEOL 2000F and Philips TEM CEM-200 FEG were available. In the Figures we have given the mean values and standard deviations of the cluster diameters. The HRTEM experiments were carried out using an acceleration voltage of 200 kV. The element specific analyses were performed using a built-in EDX system (EDAX). The images were taken using a CCD camera (Gatan). Susceptibilities were measured in the temperature range 4 to 300 K using a MPMS-XL5-SQUID magnetometer (Quantum Design), the applied magnetic field was 1 T. Data were corrected for the diamagnetic contribution of the sample holder. XPS measurements were performed on an ESCALAB 200x. $Al_{K\alpha}$ radiation ($h\nu = 1486.6$ eV) was used as excitation source.

The synthesis of the phosphane ligand was carried out under a dry nitrogen atmosphere using Schlenk technique according to the procedure outlined by Roundhill and co-workers.[15] The detailed synthesis procedure as well as NMR spectroscopic data are given in the Supporting Information. The reaction vessels used for cluster synthesis were cleaned using aqua regia to eliminate any metallic impurities.

2: A solution of Na_2-**1**$\cdot 2\,H_2O$ (0.30 g, 0.80 mmol) in methanol (20 mL) was added to a stirred suspension of $[\{Rh(cod)Cl\}_2]$ (0.20 g, 0.40 mmol) in methanol (20 mL). The mixture was stirred for 20 min. The rhodium complex dissolves and NaCl precipitates causing a slight clouding. The precipitate was removed by filtration using a glass frit. The resulting solution was evaporated in vacuo to yield 0.40 g (90 %) of a powdery yellow solid. $^{31}P\{1H\}$-NMR (81 MHz, D_2O): [ABX]-spin system $\delta = 23.3$ ($^3J_{P,P} = 11.4$ Hz, P^V), 22.2 ppm ($^3J_{P,P} = 11.4$ Hz, P^{III}; $^1J_{P,Rh} = 154.8$ Hz, P^{III}); ^1H NMR (500 MHz, CD_3OD): $\delta = 7.8$–7.3 (m, 10 H; C_6H_5), 5.5–5.0 (m, 2 H; CH *trans* to P), 2.9–2.7 (m, 2 H; CH *trans* to O), 2.5–1.7 ppm (m, 12 H; CH_2); IR (KBr): $\tilde{\nu} = 3421$ br, 3054 w, 2918 w, 1632 br, 1483 s, 1435 m, 1159 s, 1099 m, 1041 s, 744 m, 696 cm^{-1} s; MS (FAB^+, NBA): *m/z* 527 (73.6, $[M+H]^+$), 549 (7.5 % $[M+Na]^+$.

Rhodium cluster (6 nm): **2** (0.16 g, 0.30 mmol) was dissolved in water (15 mL). The solution is stirred at ambient temperature for 2–

3 days under atmospheric hydrogen pressure. The initially yellow solution turned brown after a few hours and then black. The rhodium clusters were isolated as a black solid after evaporation of the solution. To remove excess ligands, the black solid is resuspended in ethanol (10 mL) by using an ultrasonic bath. Over night the clusters precipitate. After centrifugation and drying the rhodium clusters were isolated as a black shiny powder which readily dissolved in water. This work-up procedure was repeated until no more ligand signals were seen in the ^{31}P NMR spectrum of the centrifugate.

Received: August 19, 2006
Published online: December 27, 2006

Keywords: biphasic catalysis · clusters · phosphonic acid · rhodium · transmission electron microscopy

---

[1] a) *Nanoparticles. From Theory to Application* (Ed.: G. Schmid), Wiley-VCH, Weinheim, **2003**; b) *Clusters and Colloids: From Theory to Application* (Ed.: G. Schmid), VCH, Weinheim, **1994**; c) B. F. G. Johnson, *Coord. Chem. Rev.* **1999**, *190–192*, 1269–1285; d) G. Schmid, *Chem. Rev.* **1992**, *92*, 1709–1727; e) G. Schmid, *Mater. Chem. Phys.* **1991**, *29*, 133–142; f) B. C. Gates, *Chem. Rev.***1995**, *95*, 511–522; g) A. Roucoux, J. Schulz, H. Patin, *Chem. Rev.* **2002**, *102*, 3757–3778.

[2] L. N. Lewis, *Chem. Rev.* **1993**, *93*, 2693–2730.

[3] W. F. Maier, *Angew. Chem.* **1989**, *101*, 135–146; *Angew. Chem. Int. Ed. Engl.* **1989**, *28*, 135–145, and references therein.

[4] J. Schulz, A. Roucoux, H. Patin, *Chem. Commun.* **1999**, 535–536.

[5] H. Bönnemann, W. Brijoux, *Adv. Catal. Nanostruct. Mater.* **1996**, 165–196, and references therein.

[6] a) E. G. Kuntz, *Chemtech* **1987**, *17*, 570–575; b) T. G. Southern, *Polyhedron* **1989**, *8*, 407–413; c) M. Barton, J. D. Atwood, *J. Coord. Chem.* **1991**, *24*, 43–67; d) P. Kalck, F. Monteil, *Adv. Organomet. Chem.* **1992**, *34*, 219–284; e) W. A. Herrmann, C. W. Kohlpaintner, *Angew. Chem.* **1993**, *105*, 1588–1609; *Angew. Chem. Int. Ed. Engl.* **1993**, *32*, 1524–1544.

[7] J. Podlahova, B. Kratochvil, V. Langer, *Inorg. Chem.* **1981**, *20*, 2160–2164.

[8] J. C. Jeffrey, T. B. Rauchfuss, *Inorg. Chem.* **1979**, *18*, 2658–2666.

[9] O. Krampe, C.-E. Song, W. Kläui, *Organometallics* **1993**, *12*, 4949–4954.

[10] As expected on the basis of the pK_a values of the phosphonic acid, the clusters precipitate when the pH value of the solution sinks below 6. The clusters also coagulate upon addition of tap water. When edta (ethylenediamine tetraacetate) solution is added, the clusters redissolve. Phoshonic acids form sparingly soluble salts with divalent cations, such as magnesium and calcium.

[11] C. Larpent, R. Dabard, H. Patin, *Inorg. Chem.* **1987**, *26*, 2922–2924.

[12] a) S. Burnet, T. Yonezawa, J. J. van der Klink, *J. Phys. Condens. Matter* **2002**, *14*, 7135–7145; b) C. Barreteau, R. Guirado-López, D. D. Spanjaard, M. C. Desjonquères, A. M. Olés, *Phys. Rev. B* **2000**, *61*, 7781–7794; c) Z.-Q. Li, J.-Z. Yu, K. Ohno, Y. Kawazoe, *J. Phys. Condens. Matter* **1995**, *7*, 47–53; d) A. J. Cox, J. G. Louderback, S. E. Apsel, L. A. Bloomfield, *Phys. Rev. B* **1994**, *49*, 12295–12298.

[13] For a discussion upon the various factors determining XPS energies of metallic nanoparticles see I. Lopez-Salido, D. C. Lim, R. Dietsche, N. Bertram, Y. D. Kim, *J. Phys. Chem. B* **2006**, *110*, 1128–1136, and references therein.

[14] M. P. Seah, W. A. Dench, *Surf. Interface Anal.* **1979**, *1*, 2–11.

[15] S. Ganguly, J. T. Mague, D. M. Roundhill, *Inorg. Chem.* **1992**, *31*, 3500–3501.